Fuel Processing Technology 140 (2015) 46–56

Contents lists available at ScienceDirect

Fuel Processing Technology

journal homepage: www.elsevier.com/locate/fuproc

Research article

Evaluating the pelletization of "pure" and blended lignocellulosic biomass feedstocks

Nathan C. Crawford [a,*], Allison E. Ray [b], Neal A. Yancey [b], Nick Nagle [a]

[a] National Bioenergy Center, National Renewable Energy Laboratory, Golden, CO 80401, USA
[b] Biofuels and Renewable Energy Technology, Idaho National Laboratory, Idaho Falls, ID 83415, USA

ARTICLE INFO

Article history:
Received 30 March 2015
Received in revised form 18 August 2015
Accepted 20 August 2015
Available online xxxx

Keywords:
Biomass
Feedstock
Pelleting
Blending
Flowability
Shear
Powder rheometer
Compressibility
Yield stress
Friction

ABSTRACT

Due to its low density and poor flowability, raw biomass may not be an economically viable feedstock for the production of biofuels. However, mechanical densification can be employed to improve its viability. In this study, the flow properties (compressibility, shear, and wall friction) of "pure" feedstocks (corn stover, hybrid poplar, switchgrass and *Miscanthus*), and feedstock blends, are investigated and compared to measured pelleting energy consumption values. As anticipated, the more compressible materials required lower pelletization energies. Conversely, the less flowable feedstocks (i.e., the materials with higher cohesion and yield strength) were less energy intensive to pellet. In addition, the flowability parameters of the blended materials could be predicted by averaging the measured flow parameters of their pure feedstock constituents. Therefore, only the flow characteristics of the pure feedstocks need to be directly measured, while the flowability of a blended feedstock with a known blend ratio can be accurately inferred. A model was also developed to calculate the required pressure to pellet a particular feedstock, pure or blended, based on its flowability parameters (namely compressibility and wall friction). Strong correlation was observed between the measured pelleting energy consumption and the predicted pelleting pressure values. This newly developed model allows for a material's pelleting feasibility to be assessed without having to physically pelletize the material.

Published by Elsevier B.V.

1. Introduction

The conversion of biomass, specifically lignocellulosic biomass, into liquid transportation fuels (i.e., biofuels) has the potential to provide renewable alternatives to those derived from fossil carbon sources (such as oil, natural gas, and coal). Lignocellulosic (LC) biomass is the fibrous, structural portion of plants; common examples include: crop residues such as corn stover and bagasse, and energy crops like switchgrass and poplar [1]. In addition, LC biomass is the most abundant source of renewable carbon on the planet [2] and is not suitable for human consumption, completely eliminating the food-to-fuel paradigm.

A consistent supply of a high-quality, economical feedstock is critical to achieving national biofuel goals; however, raw biomass is not an economically viable feedstock. The major disadvantage of raw biomass is its low bulk density, which typically ranges from 40 to 100 kg/m^3 for agricultural grasses and straws, and 150 to 250 kg/m^3 for woody resources [3,4,5,6]. As a result, the low densities of biomass often make it difficult to store, transport, and interface with biorefinery infeed systems [3,5,7].

However, "loose" biomass can be mechanically densified into pellets, increasing bulk density as much as ten-fold [3], with reported final compaction densities of 600 to 1200 kg/m^3 [8,9,10,11,12,4]. Mechanical densification not only leads to improved bulk density, but it also enhances feedstock durability, storability, and uniformity [3]. Additionally, "loose" biomass is known for its poor flowability which prevents it from flowing properly during discharge and transfer through biorefinery operations. As a result, biorefineries would need to install specialized equipment to handle these materials, making retrofitting existing corn-based ethanol plants into cellulosic ethanol plants complicated and costly [13]. The uniform size and shape of pelleted biomass, on the other hand, make it more compatible with existing grain-based storage and handling equipment [14].

Yet, high energy consumption values have kept pelletization from being used for large-scale biofuel production. The energy costs during grinding and pelleting of biomass would need to be less than the gained savings from enhanced transportation and storage efficiency [13]. Energy requirements for the densification of biomass will depend heavily on the applied pressure, as well as the method of compaction. Also, pelleting energy is contingent on the physical properties of the material being compressed, such as (but not limited to) moisture content, particle size and size distribution, and initial bulk density [5].

Although difficult to quantify, a recent study by Wilson et al. [13] investigated the costs associated with the processing, transportation, and storage of baled versus pelleted biomass. They estimated the costs for pelleting a variety of feedstock species to be around $30/t. Using data from Hess et al. [15], they approximated baling costs to be about $20/t

* Corresponding author.
E-mail address: nathan.crawford@nrel.gov (N.C. Crawford).

http://dx.doi.org/10.1016/j.fuproc.2015.08.023
0378-3820/Published by Elsevier B.V.

Nomenclature

A_1	Integration constant (kPa/m)
C	Compressibility (%)
C_P	Compressibility required for pelleting (%)
D	Pellet die diameter (in)
E_C	Electrical energy consumption during pelleting (kWh/t)
f_c	Unconfined yield stress (kPa)
ff_c	Flowability (or flow) index, $=\sigma_1/f_c$ (−)
κ	Radial-to-axial stress proportionality constant, $=\sigma_1/\sigma_2$ (−)
L	Pellet die length (in)
L/D	Pellet die length-to-diameter ratio (−)
μ_w	Coefficient of wall friction (−)
MC	Moisture content (%)
N	Normal stress (kPa)
Nc	Pre-shear critically consolidated normal stress (kPa)
P	Pressure (MPa)
P_C	Compression pressure (MPa)
P_P	Pelleting pressure (MPa)
P_w	Wall pressure (MPa)
ϕ_i	Angle of internal friction (°)
ϕ_e	Effective angle of internal friction (°)
r	Radial coordinate (−)
R	Pellet die radius (in)
ρ_P	Pellet bulk density (g/mL)
ρ_G	Ground (or "loose") bulk density (g/mL)
σ_1	Major principal stress (kPa)
σ_2	Minor principal stress (kPa)
τ	Shear stress (kPa)
τ_0	Cohesion (kPa)
z	Axial coordinate (−)

(a net difference of $10/t). However, the reduced transportation and storage costs for pelleted biomass accounted for an average savings of $50/t compared to baled biomass [13]. Therefore, the reduced truck traffic and increased conveying and storage efficiencies substantially offset any additional processing costs associated with pelleting; making biomass pelletization an economical and intriguing pre-processing option.

Beyond bulk density, another challenge with using raw biomass as a feedstock is the necessity to create a reliable year-round feedstock supply. Feed crops are region and climate specific, and as a result, they are harvested at different times of the year (such as cool season grasses in early spring, wheat, barley and oat straw during the summer, corn and grain sorghum stalks in the fall, and perennial grasses such as switchgrass in the early winter) [13]. In order for a biorefinery to have a consistent feedstock supply and composition, massive storage facilities would be required. Pelleting could reduce storage volume requirements by a factor of two compared to the volumes required for "loose," non-pelleted biomass [16]. However, due to different harvest times, multiple biomass species would need to be fed and/or pelleted simultaneously to keep a uniform feedstock composition.

The blending of time-dependent and location-specific materials would enhance supply-chain efficacy and stabilize feedstock compositional variance. Feedstock blends can be formulated not only based on availability, but with the intention to target specific physiochemical characteristics (such as reduced milling energy requirements, increased digestibility, reduced ash formation, and improved flowability properties). For instance, switchgrass required ~3-times more energy (on average) to hammer mill relative to corn stover [6]. While woody feedstocks, like hybrid poplar or pine, tend to result in lower ash formation in comparison to herbaceous feedstocks, such as corn stover and switchgrass [17,18,19]. A material like corn stover can be blended with other biomass to reduce milling energy requirements; however, in order to keep ash content low, a woody biomass could be added to counter balance increased ash formation. Therefore, in addition to pelleting, biomass blending and formulation will be essential to achieving sustainable biofuel production [17].

A number of studies have investigated the densification of herbaceous and woody biomass materials. Ndiema et al. [20] examined the influence of die pressure on the relaxation characteristics of briquetted rice straw, while Adapa et al. [9] studied the specific energy required to pelletize barley, canola, oat, and wheat straws. Li and Liu [21] used a punch-and-die process to densify wood residues into fuel-grade slugs and Mani et al. [5] evaluated the compaction mechanism of straws, corn stover and switchgrass at different compression forces, particle sizes, and moisture contents. In addition, several studies have investigated the impact of particle size and moisture content (among others) on the physical properties of pelleted biomass [22,23,24,14,25]. More recently, Monedero et al. [26] studied the effects of material composition, additive concentration, moisture content, and compression on the pelletization process and pellet quality of "pure" and blended pine and poplar sawdust.

However, to our knowledge, no study has used flow measurements (compressibility, yield strength, wall friction, etc.) to directly predict the pelletization of pure and blended biomass feedstocks. Knowledge of how the compaction and flow properties of different biomass species correlate with the pelletization process will allow scientists to forecast whether or not a feedstock is suitable for pelleting, and lead to improved feedstock blend formulation prior to pelleting.

The objectives of this study were to (1) investigate the flow properties of pure feedstock species, (2) compare the flow properties of the pure species to the flowability measurements of feedstock blends, (3) use the flow properties of the feedstocks, both pure and blended, to predict pelleting pressure requirements, and (4) compare the pelleting pressure predictions to measured pelleting energy consumption values.

2. Materials and methods

2.1. Materials

The lignocellulosic biomass feedstocks selected for this study include: corn stover (CS), hybrid poplar (HP), switchgrass (SG), and *Miscanthus* (MIS) (Fig. 1). These materials provide a robust mix of herbaceous and woody plants. More specifically, corn stover, switchgrass, and hybrid polar were chosen because they represent a combination of crop residue, energy crop, and hardwood species.

Single-pass corn stover was harvested in October 2012 in Ames, IA. Bales of corn stover were received at INL in December 2013. Clean chips of hybrid poplar were obtained from Boardman, OR in November 2013. Switchgrass was harvested from Garvin county, OK and collected by Oklahoma State University in July 2012, and switchgrass bales were received in November 2013. *Miscanthus* was harvested from Tifton, GA in January 2014, and super sacks of chopped, 1-in. material were shipped to INL in February 2014.

Bales of corn stover and switchgrass, chopped *Miscanthus*, and chips of hybrid poplar were fed through a two-stage, full-scale grinding process for the purpose of pelleting using the Feedstock Process Demonstration Unit (PDU) as part of DOE's Biomass Feedstock National User Facility (BFNUF) that is located at Idaho National Laboratory (Idaho Falls, ID). First, material was processed through a Vermeer BG-480 (Pella, IA), which has two horizontal grinding drums with swinging hammers powered by two, 200-HP motors [27], and passed through a 2-in. screen. Then, the 2-in. screened material was processed through a Bliss hammer mill (Ponca City, OK) with a 1/4-in. screen. Two, 5-gal buckets of ground material were sent to the National Renewable Energy Laboratory (Golden, CO) for further studies. The two-stage grinding process discussed here was employed solely for generating material for pelleting and is not a typical milling method used for the conversion of "loose" biomass to fuels.

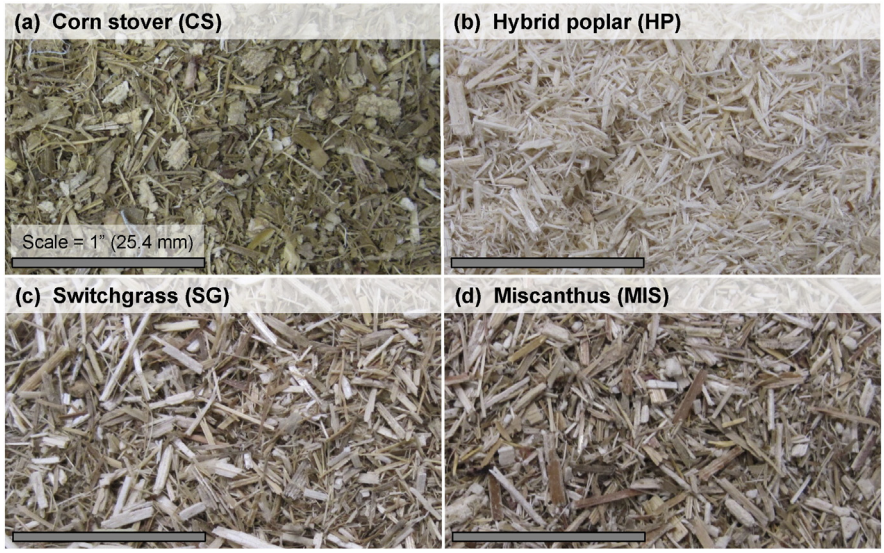

Fig. 1. Digital images of: a) corn stover, b) hybrid poplar, c) switchgrass, and d) *Miscanthus* feedstocks (scale bar = 1 in.).

The ground "pure" feedstock species were blended into one binary and two ternary blend formulations on a dry weight basis. The binary blend was a 50:50 wt.% mix of CS and SG, while the ternary blends were 33:33:33 wt.% combinations of CS + SG + HP and CS + SG + MIS. Blending ratios can be designed to target a specific composition (e.g., to adjust glucan, xylan, and lignin fractions), and to enhance digestibility and limit ash content.

2.2. Pelleting

Ground biomass was pelleted using a Bliss Pioneer Pellet Mill (B35A-75) at Bliss Industries, LLC testing laboratory (Ponca City, OK). The mill has a rated output of ~1000 kg/h for herbaceous biomass, although capacity is material dependent. The pellet mill has two, 40-HP motors, and each motor is instrumented to measure current for calculation of electrical energy consumption. The die length-to-diameter ratio (L/D) was selected based upon the feedstock or blend being processed. Pellets were produced for each feedstock and the three blendstocks (Table 1). Pellet durability was measured and validated, but results are not reported here.

2.3. Particle sizing

Super sacks of ground biomass were sent to Bliss Industries, LLC. Sieve analysis and bulk density measurements were performed at the Bliss test lab. The moisture content and bulk density were measured for both the ground and pelleted materials (Table 1). All feedstock material (pure and blended species) were sieved to obtain particle classifications across fourteen size ranges (in μm): <74, 74–104, 104–150, 150–178, 178–211, 211–297, 297–419, 419–594, 594–841, 841–1191, 1191–1679, 1679–2380, 2380–3353, and >3353. After sieving, the mass retained on each sieve was weighed. The geometric average particle size and standard deviation were calculated according to ISO standard 9276-2:2014 [28].

The sieve sizing data were corroborated and expanded upon using optical microscopy (Leica DM 3000, Clemex Technologies Inc., Longueuil, Quebec, Canada; data analysis via Clemex Vision PE software, version 6) at NREL. The optical micrographs not only allowed for sizing of the feedstock materials, but also particle dimensional analysis, namely aspect ratio. To expedite the analysis process, only the pure feedstock species (CS, HP, SG, and MIS) were evaluated optically. Average particle dimensions obtained via microscopy were reported on a volume basis [29,28]. Analyzing microscopy results on a volume basis allows for a more direct comparison between other commonly used biomass sizing techniques (i.e., sieving and/or laser diffraction).

2.4. Powder rheometer

The FT4 Powder Rheometer (Freeman Technology, Worcestershire, UK) was used at NREL to measure the flow properties of the pure and blended biomass feedstocks. The FT4 Powder Rheometer is a universal powder tester, with accessories for measuring compressibility and rotational shear properties, including wall friction (the FT4 has additional testing methodologies that were not employed for this study). A full description of the FT4's capabilities can be found elsewhere [30,31].

All testing were done using the 50 mm diameter, borosilicate test vessel (85 mL test volume). In order to standardize the packing state of each sample before testing, all samples were conditioned using the 23.5 mm blade (the biomass particles become entangled with the larger blades leading to a torque overload). The conditioning protocol consists

Table 1
Biomass pelleting parameters and results, where: MC is the moisture content, ρ is the density, L is the pellet die length, L/D is the pellet length-to-diameter ratio ($D = 0.25$ in.), and E_C is the electrical energy consumption during pelleting. The "±" indicates a single standard deviation from (at minimum) triplicate measurements.

Material	MC (%)		ρ (kg/m^3)		L	L/D	E_C
	Ground	Pellet	Ground	Pellet	(in)	(−)	(kWh/ton)
CS	11.63 ± 0.05	6.66 ± 0.03	112 ± 3	695 ± 3	3.00	12	88
HP	13.52 ± 0.03	8.58 ± 0.02	117 ± 2	650 ± 17	2.25	9	107
SG	12.62 ± 0.03	7.17 ± 0.03	128 ± 2	610 ± 4	2.50	10	146
MIS	13.21 ± 0.04	9.22 ± 0.03	144 ± 3	658 ± 25	3.00	12	293
CS + SG	10.71 ± 0.06	7.14 ± 0.02	115 ± 16	670 ± 10	2.25	9	79
CS + SG + HP	11.13 ± 0.09	8.47 ± 0.02	128 ± 2	642 ± 14	2.25	9	100
CS + SG + MIS	10.16 ± 0.03	8.62 ± 0.02	133 ± 1	627 ± 4	2.25	9	78

of an axial traverse of the blade downward and upward through the entire height of the sample. During the upward traverse, the blade lifts each particle and gently drops them behind the blade. Conditioning loosens and slightly aerates the granular sample, removing any packing history such as excess trapped air or pre-consolidation either from storage or during filling of the vessel.

All test sequences, compressibility, shear cell, and wall friction, were repeated in triplicate (at minimum) to assess measurement reproducibility, with all error bars reported as a single standard deviation.

2.4.1. Compressibility

During the compressibility test, the pre-conditioned sample bed is compressed with a vented piston that allows entrained air to escape. Each sample is slowly compacted across a range of normal stresses (N) from 0.5 to 21 kPa, measuring the change in bed height at 11 distinct intervals. The compressibility of a sample (C) is defined as the percent change in volume after compression, $C = (V_0 - V)/V_0$; where V_0 is the initial, conditioned volume and V is the volume at a specific normal stress value.

2.4.2. Shear cell

Shear cell tests were performed with the 48 mm shear head in the force control mode, so as the shear head was rotated, the torque signal was measured while the normal force was held constant (i.e., the shear head can displace vertically during testing). During the shear cell test, the sample is first compacted with the vented piston to a specified pre-shear normal load (3, 6, 9, or 15 kPa). After compaction, the piston is removed and the shear head is attached. The shear head is then lowered, inserting its blades into the sample until the pre-shear normal force is again established. The head is then slowly rotated, inducing a shear stress. The sample is continuously sheared until the shear stress reaches steady state and the sample is "critically consolidated" [32]. Next, the normal stress is reduced, allowing room for the particles to dilate and move past one another. At this point, a yield stress can be measured. The pre-shear/shear sequence is repeated five times (as recommended by Carson and Wilms [33]) at decreasing normal stress values (the sample is always pre-sheared to the critically consolidated state before measurement). A curve of the normal stress and shear stress pairings is then obtained, referred to as the yield locus. A yield locus is unique and contingent on its pre-shear history. The yield loci were individually evaluated using Mohr stress circle analysis to acquire values of: the major and minor principal stress, unconfined yield strength, cohesion, and interparticle friction, as described by Carson and Wilms [33] and Freeman [30].

To characterize the flowability of a material, Jenike [32] proposed to use the ratio of the major principal stress to the unconfined yield strength, called the flowability index (ff_c). Based on the flow index value, a material can be classified as non-flowing, very cohesive, cohesive, easy flowing, or free flowing (Table 2) [34].

2.4.3. Wall friction

Wall friction properties are vital for understanding how a consolidated granular material will interact with the wall material of its container or processing equipment. Wall friction tests are nearly identical to the shear cell testing. Instead of shearing the sample against itself and obtaining interparticle properties like interparticle friction or cohesion, the wall friction test shears the sample against a metallic disc with well defined material properties. In essence, the shear head is replaced with a 48 mm stainless steel coupon (316 grade, 1.2 μm surface roughness). During wall friction testing, the sample is compacted and pre-sheared at a specified normal stress load (3, 9, or 15 kPa). Once again, the normal force is decreased and the sample is sheared until failure. The shear stress and normal force pairs are plotted to obtain a wall friction yield locus. Wall friction coefficients, or angles, can be extracted from the loci. Since the structural integrity of the sample is not disrupted during shearing, the wall friction test requires only one pre-shear step and five subsequent shear steps.

Table 2
Classification of granular solids flowability via flowability index.

Non-flowing	Very cohesive	Cohesive	Easy flowing	Free flowing
$ff_c < 1$	$1 < ff_c < 2$	$2 < ff_c < 4$	$4 < ff_c < 10$	$ff_c > 10$

3. Results and discussion

3.1. Particle sizing

The particle size distributions of the pure feedstocks via sieving are similar and do not appear to be significantly different (Fig. 2). The sieved geometric average particle sizes of CS, HP, SG, and MIS were 990, 1068, 934, and 991 μm, respectively. Although not plotted in Fig. 2 (for clarity), the geometric average particle sizes of the blendstocks CS + SG, CS + SG + HP, and CS + SG + MIS were respectively 935, 987, and 971 μm. Again, a distinct difference between the sieved average particle sizes and size distributions for the pure and blended feedstocks was not observed.

However, the breadth of the particle size distributions appear to be different for the pure feedstocks. More specifically, the smallest sieve openings (pan, 74, and 104 μm) and the largest sieves (2380 and 3,353 μm) display the greatest discrepancy in particle weight fraction across the different feedstock materials (Fig. 2). Thus, the weight fraction of fines (defined for this study as the particles <150 μm) and coarse particles (defined as the particles >2380 μm) were summed for each pure and blended feed species (Fig. 3). Both CS and HP have the greatest amount of coarse particles, with weight fractions >4%. SG and MIS, on the other hand, have weight fractions of coarse particles of 0.7 and 1.5%, respectively. In addition, HP, SG, and MIS also have low fractions of fines (correspondingly 0.6, 1.0, and 0.3%), while CS has the greatest amount of fine particles at 1.6%. Therefore, CS has the broadest size distribution of all the pure feedstock materials, while SG and MIS have distributions that are relatively narrow (with the low amounts of fine and coarse particles). Materials with broader size distributions have commonly been found to be more compressible and less flowable [6,35]. Alternatively, HP has a particle size distribution biased towards large particles, with a substantial amount of coarse particles and a low amount of fines.

The feedstock blends have elevated levels of both coarse and fine particles (Fig. 3). All three blendstocks have weight fractions of coarse particles of ~3.3% (still less than the amount of coarse particles found

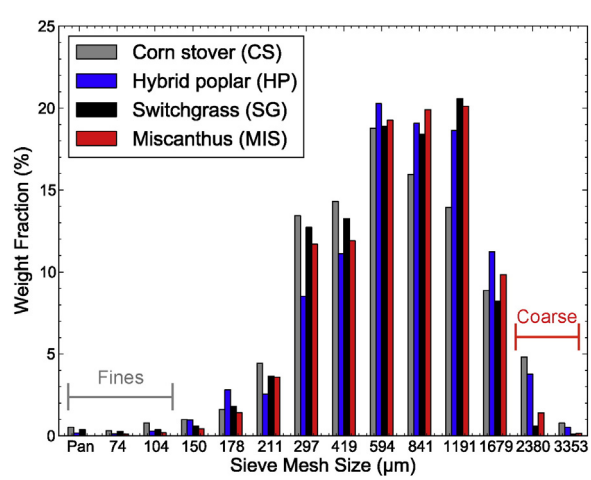

Fig. 2. Size distribution of corn stover (gray), hybrid poplar (blue), switchgrass (black), and *Miscanthus* (red) feedstocks using standard US mesh sieves. (For interpretation of the references to color in this figure legend, the reader is referred to the web version of this article.)

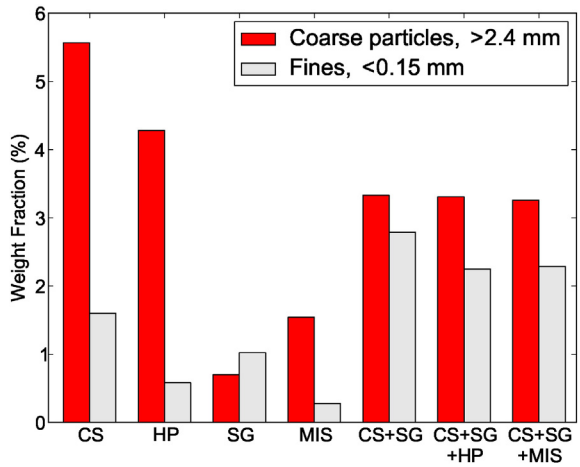

Fig. 3. Weight fraction of coarse (>2.4 mm) and fine (<0.15 mm) particles for the pure and blended feedstocks.

in CS and HP). However, all three feedstock blends have significantly more fine particles (> 2%) than the pure feedstocks; which is not reasonable, but most likely stems from a sampling issue at the time of sieving (e.g., perhaps the blend materials were stored differently, or were sampled from a different part of the storage container, or not fully homogenized prior to sieving). Nonetheless, the large amount of fines within the blendstocks would make them less compressible, while the moderate amount of coarse particles would enhance compressibility [6]. Therefore, it is expected that the blended feedstocks will be moderately compressible compared to the pure feedstock species.

The volume-based average particle length for the four pure feedstock species ranged from ~1000 to 1500 μm (Table 3), with CS displaying the smallest average length. HP and MIS had the largest average particle lengths at ~1500 μm. CS also had the smallest average particle width at 436 μm, while HP had the largest average particle width at 719 μm. However, the large variance in the length and width values keep them from being statistically unique between the different feedstocks. Additionally, the particle length values agree with the average particle size values from the sieving data. Therefore, the two separate sizing techniques corroborate one another.

The optical microscopy results also allow for the measurement of particle aspect ratio (defined as the length to width ratio). The average aspect ratio is between 2 to 3 for all four of the feedstocks, with a maximum value of 10–13 (parentheses in Table 3). Thus, both sizing techniques (sieving and microscopy) indicate that the grinding of the feedstocks was consistent across the different species. In addition, the aspect ratios of the ground feedstocks evaluated here were much smaller than typically observed with milled biomass. As a result, the ground species should experience less interparticle entanglements and be more flowable than coarsely milled materials. Although microscopy allowed for examination of particle shape, the sieving analysis allowed for more effective analysis of the particle size distributions (i.e., fine versus coarse particles).

Table 3
Volume-based average particle dimensions via optical microscopy (n = the number of particles sized). The "±" values are a single standard deviation, while the values in the parentheses indicate a maximum measured aspect ratio.

Feedstock	n (−)	Length (μm)	Width (μm)	Aspect ratio (−)
CS	4432	984 ± 532	436 ± 201	2.2 (10.4)
HP	4430	1522 ± 714	719 ± 324	2.7 (10.9)
SG	3117	1250 ± 695	547 ± 342	2.9 (13.0)
MIS	2781	1523 ± 680	568 ± 297	2.9 (12.8)

3.2. Compressibility

Compressibility is a bulk property measurement that indicates a material's ability to become compacted when subjected to a normal force. The compressibility test is not a direct measurement of flowability, but it can indicate the strength of adhesive forces between particles.

The compressibility of the pure (Fig. 4) and blended (Fig. 5) feedstocks was assessed from 0.5 to 21 kPa. When considering the compressibility of the four pure feedstocks, the CS sample was the most compressible, compressing by 38% at 21 kPa (Fig. 4). HP was slightly less compressible (compressing 32% at 21 kPa), while SG and MIS were the least compressible (compressing 28 and 27%, respectively, at 21 kPa). Interestingly, the more compressible materials (CS and HP) are also the materials that required less energy during the pelleting process (Table 1). Conversely, the least compressible materials (SG and MIS) required the most energy during pelletization. Therefore, there is a direct relationship between compressibility and pelletization energy.

The additional compressibility of corn stover and hybrid poplar is most likely due to both differences in material structure and size distribution. Corn stover is a heterogeneous material with a low fiber content and the vascular tissues that makeup its stalk are more spongy [6]. Therefore, it is expected to be more compressible than the other materials studied here. *Miscanthus* and switchgrass are more fibrous and rigid, while hybrid poplar is a hardwood known for its flexibility. It is reasonable to assume that the hybrid poplar sample would be more compressible than the fibrous grassy materials, *Miscanthus* and switchgrass.

Furthermore, in comparison to the SG and MIS samples, CS and HP both have a significant fraction of large particles (>2.4 mm), 5.5 and 4.2% w/w, respectively; while the SG and MIS both have weight fraction of large particles less than 2% (Fig. 3). Additionally, the CS sample has more fines (1.7 wt.% particles <0.15 mm) than the other pure feedstocks (all with <1%). The large particles in the CS and HP samples create collapsible void spaces in the solids network. During compaction, smaller (fine) particles rearrange and fill in the void spaces surrounding the larger (coarse) particles [35,36]. As a result, materials with broader size distributions are typically more compressible [6,35].

The three blended feedstocks, on the other hand, had nearly identical compressible behaviors, with compressibilities of 31, 32, and 33% at 21 kPa for the CS + SG, CS + SG + MIS, and CS + SG + HP, respectively. The compressibilities of the feedstock blends overlap with the HP sample, the more moderately compressible pure feedstock.

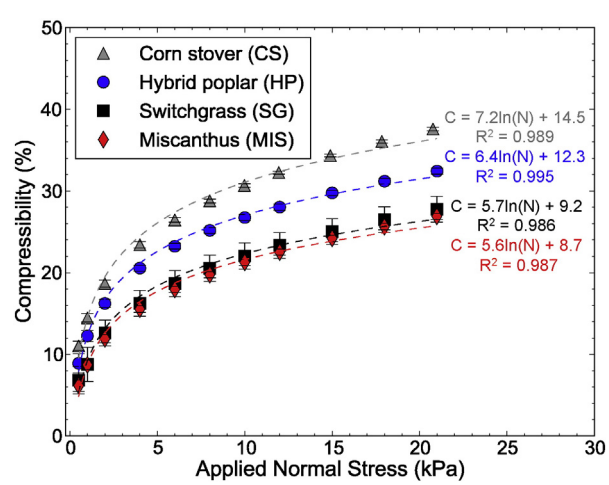

Fig. 4. Compressibility (% change in volume) of corn stover (triangles), hybrid poplar (circles), switchgrass (squares), and *Miscanthus* (diamonds) feedstocks as a function of applied normal stress. The dashed lines are logarithmic fits to the individual data sets.

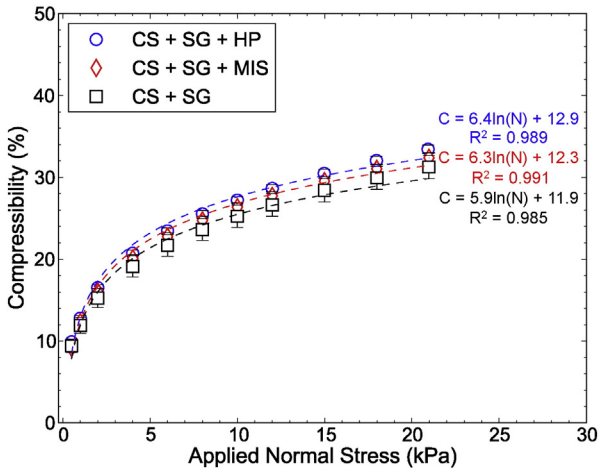

Fig. 5. Compressibility (% change in volume) of blended feedstocks: CS + SG (open squares), CS + SG + HP (open circles), and CS + SG + MIS (open diamonds) as a function of applied normal stress. The dashed lines are logarithmic fits to the individual data sets.

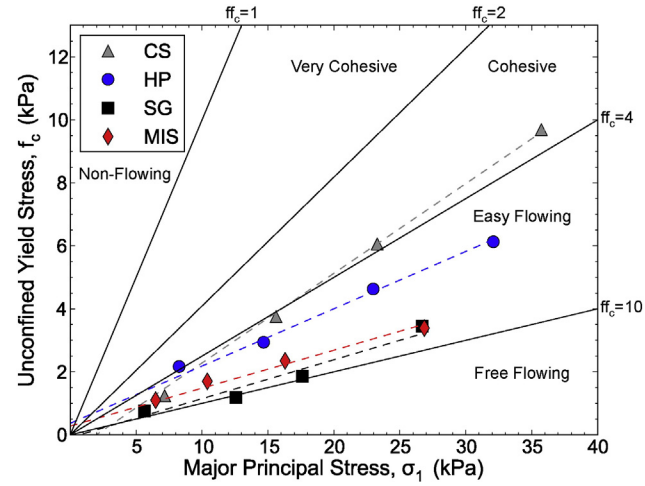

Fig. 7. Unconfined yield stress versus major principal stress for corn stover (triangles), hybrid poplar (circles), switchgrass (squares), and *Miscanthus* (diamonds) feedstocks. The solid lines represent the boundaries between flowability designations, while the dashed lines are linear fits to the individual data sets.

3.3. Shear testing

3.3.1. "Pure" feedstocks

Shear cell tests were designed to determine the shear stress required to initiate flow of a pre-consolidated sample of granular solids (i.e., the yield stress). Shear cell measurements indicate how easily a material will transition from a static state into dynamic flow. Originally, shear testing was used exclusively for the design of hoppers and silos, but today they are commonly used for the general characterization of granular materials.

The yield stress values for the four pure feedstocks, CS, HP, SG, and MIS, at a pre-shear normal stress value of 9 kPa were segmented into two groupings (Fig. 6). The CS and HP samples displayed relatively high and similar yield strengths, cohesion, and interparticle friction. While the SG and MIS materials had lower yet similar yield stress, cohesion, and interparticle friction values. Interestingly, the easier to pellet materials (CS and HP) are less "flowable" than the more difficult to pellet materials (SG and MIS). Therefore, there is an inverse relationship between the ease of pelleting and material flowability.

Using Mohr circle analysis, the yield loci from Fig. 6 can be assessed to produce values of the unconfined yield stress (f_c) and the major principal stress (σ_1). Plotting f_c as a function of σ_1 generates a linearized flow function, where the flowability index (ff$_c$) is the inverse of the slope. Moving counter-clockwise in Fig. 7, the values of the flowability index (given in Table 2) decrease from the free flowing region to the non-flowing regime.

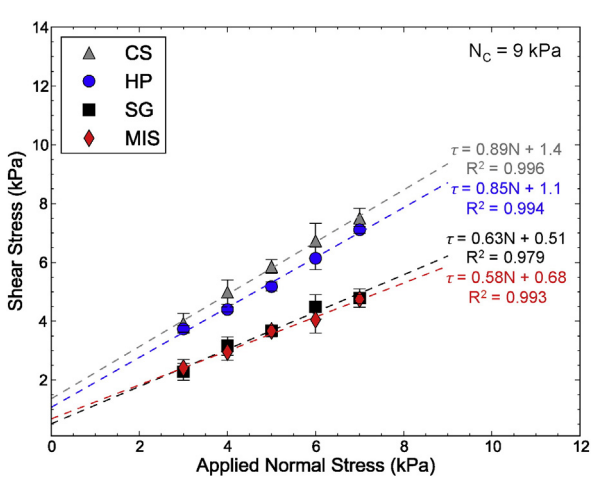

Fig. 6. Yield loci of corn stover (triangles), hybrid poplar (circles), switchgrass (squares), and *Miscanthus* (diamonds) feedstocks at a pre-shear consolidation normal stress (N_C) of 9 kPa. The dashed lines are linear fits to the individual yield loci.

The flow functions for all four pure feedstocks yielded linear increases in f_c with increasing σ_1 (Fig. 7); with HP, SG, and MIS all falling in the easy flowing region (although HP did have a significantly lower flow index than SG and MIS). Conversely, CS crossed two flow regimes with a flow index in the cohesive and easy flowing regions. At low major principal stresses, CS displays comparable flowability to MIS and SG, but as the major principal stress increases, CS becomes less flowable. At large principal stress values ($\sigma_1 > 15$ kPa), CS became distinctively the least flowable of the four pure feedstocks. Flowability is dependent on the physical properties of the material, as well as the environmental conditions and the equipment used for handling, storing, and processing [37]. Typically, only simple granular solids display consistent flowability across different stress regimes [38,39]. Therefore, corn stover is a complex material whose flow behavior increases in difficulty as the consolidation stress is increased. The complex behavior of corn stover is a direct result of its heterogeneous composition. SG, MIS, and HP are relatively homogeneous materials harvested from the same part of their respective plants. CS, on the other hand, is a varied feedstock made from mixed parts of the plant (the stock, stem, leafs, and cob).

Overall, the flow indices (ff$_c$) for the ground feedstocks in this study agree with previously reported ff$_c$ values for ground biomass species, which typically range from the easy flowing to cohesive regimes [39, 40,41]. Milled biomass materials, due to their larger particle sizes and aspect ratios (which can lead to more frequent interparticle entanglements), are usually less flowable than ground biomass, with ff$_c$ values commonly in the cohesive to very cohesive regimes [35,42].

A summary of all flowability parameters, including: unconfined yield stress (f_c), major and minor principal stresses (σ_1 and σ_2, respectively), cohesion (τ_0), static and effective angles of interparticle friction (ϕ_i and ϕ_e, respectively), and flowability indices (ff$_c$) for pre-shear normal stress (N_C) values of 3 to 15 kPa are reported in Table 4 for the four pure feedstocks. The cohesive strength of corn stover was found to be the highest, followed by hybrid poplar; while switchgrass and *Miscanthus* had the lowest, yet comparable cohesion. The average measured angles of internal friction were 41.3 ± 1.0, 40.0 ± 2.0, 34.9 ± 3.2, and 32.7 ± 3.9 for CS, HP, SG, and MIS, respectively (Table 4).

Fasina et al. [35] used an automated ring shear tester to study the flow properties of switchgrass (among other samples). They reported ϕ_i and ff$_c$ values of 41.8 ± 0.92 and 3.5, respectively. Chevanan et al. [42], on the other hand, used a custom fabricated linear shear box to determine the flow properties of chopped switchgrass and corn stover.

Table 4
Shear testing results for the "pure" feedstocks at pre-shear normal stress (N_C) values of 3, 6, 9, and 15 kPa (unconfined yield stress (f_c), major and minor principal stresses (σ_1 and σ_2, respectively), cohesion (τ_0), static and effective angles of interparticle friction (ϕ_i and ϕ_e, respectively), and flowability index (ff_c)).

Material	N_C (kPa)	f_c (kPa)	σ_1 (kPa)	σ_2 (kPa)	τ_0 (kPa)	ϕ_i (°)	ϕ_e (°)	ff_c (−)
CS	3	1.2 ± 0.2	7.2 ± 0.1	1.2 ± 0.1	0.28 ± 0.06	41.2 ± 1.1	45.2 ± 0.2	5.8 ± 1.1
	6	3.8 ± 0.3	15.6 ± 0.9	2.4 ± 0.1	0.85 ± 0.07	41.3 ± 0.7	46.8 ± 0.6	4.2 ± 0.1
	9	5.3 ± 0.3	23.3 ± 0.5	3.6 ± 0.1	1.36 ± 0.30	41.6 ± 1.3	47.8 ± 2.0	4.4 ± 0.1
	15	9.1 ± 0.5	35.7 ± 1.8	5.1 ± 0.3	2.50 ± 0.32	40.9 ± 0.8	48.0 ± 1.1	3.9 ± 0.2
HP	3	2.2 ± 0.2	8.3 ± 0.4	1.3 ± 0.1	0.51 ± 0.04	39.8 ± 0.6	45.9 ± 0.3	3.8 ± 0.4
	6	2.9 ± 0.4	14.7 ± 0.6	2.6 ± 0.1	0.70 ± 0.10	38.9 ± 0.6	44.5 ± 0.3	5.0 ± 0.5
	9	4.6 ± 0.9	23.0 ± 1.1	3.8 ± 0.2	1.07 ± 0.25	40.3 ± 3.5	45.7 ± 2.9	5.0 ± 0.8
	15	6.1 ± 0.5	32.1 ± 0.6	6.1 ± 0.1	1.51 ± 0.20	37.5 ± 2.2	45.5 ± 0.9	5.2 ± 0.1
SG	3	0.8 ± 0.1	5.6 ± 0.6	1.4 ± 0.1	0.20 ± 0.02	33.2 ± 2.4	39.6 ± 2.1	7.5 ± 0.6
	6	1.2 ± 0.2	12.6 ± 0.3	2.7 ± 0.1	0.29 ± 0.05	37.6 ± 1.1	39.8 ± 1.0	10.6 ± 1.7
	9	1.9 ± 0.3	17.6 ± 1.0	4.8 ± 0.3	0.51 ± 0.07	32.4 ± 1.9	34.8 ± 2.1	9.5 ± 0.7
	15	3.5 ± 0.6	26.7 ± 1.9	6.5 ± 0.5	0.95 ± 0.15	32.3 ± 1.7	36.2 ± 1.7	7.7 ± 0.9
MIS	3	1.1 ± 0.1	6.5 ± 0.7	1.3 ± 0.1	0.27 ± 0.03	37.0 ± 2.8	41.7 ± 2.5	5.9 ± 1.6
	6	1.7 ± 0.2	10.4 ± 0.2	2.9 ± 0.1	0.50 ± 0.05	28.8 ± 2.3	32.8 ± 2.3	6.1 ± 0.5
	9	2.3 ± 0.1	16.3 ± 0.6	4.6 ± 0.2	0.68 ± 0.04	30.0 ± 1.2	33.7 ± 1.4	6.9 ± 1.4
	15	3.4 ± 0.3	26.9 ± 1.7	6.1 ± 0.4	0.88 ± 0.07	35.0 ± 2.4	34.5 ± 2.1	7.9 ± 1.4

They reported ϕ_i values of 39–46 and 46–50 and ff_c values of 2.3–4.3 and 2.2–3.4 for switchgrass and corn stover, respectively. While Gil et al. [40] used a Jenike shear device to measure the flowability of poplar and corn stover milled to target particle sizes of 2 and 5 mm with varying moisture contents (7–33% w/w). They reported ϕ_i and ff_c values of 26–33 and 3.6–10.1 for corn stover and 30–32 and 3.9–12.0 for poplar. To our knowledge, there are no reported flowability data for *Miscanthus* in current literature. Even though the environmental conditions and the equipment used for handling, storing, and processing these materials varied significantly across this assortment of studies, the flow properties reported here for CS, HP, and SG coincide with published literature values.

3.3.2. Blended feedstocks

The four pure feedstocks were combined to create three feedstock blends: CS + SG, CS + SG + HP, and CS + SG + MIS (50:50 ratio by weight for the binary blend and 33:33:33 ratio for the ternary blends). The yield stress values at a pre-shear normal stress of 9 kPa for the three feedstocks were nearly identical (Fig. 8). The CS + SG and CS + SG + HP blends both had cohesive strengths of ~1 kPa and interparticle friction angles of ~38; while the CS + SG + MIS sample had a cohesion stress and interparticle friction angle of 0.7 kPa and 36, respectively. The yield loci of the blended feedstocks fall directly between the measured yield loci of the pure feedstocks in Fig. 6; indicating that flow properties can be tuned via feedstock blending.

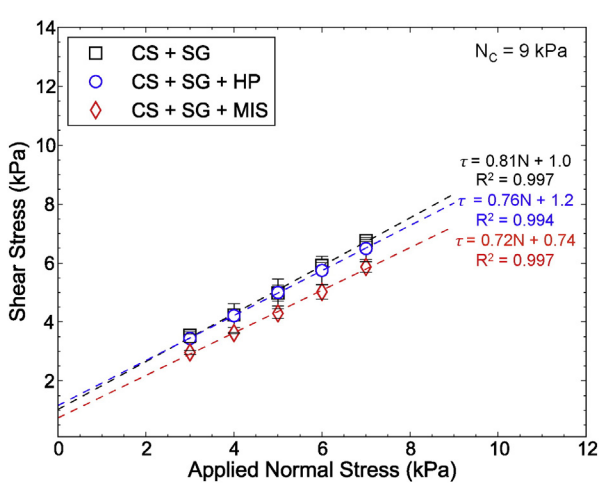

Fig. 8. Yield loci at a pre-shear consolidation normal stress (N_c) of 9 kPa for blended feedstocks: corn stover + switchgrass (squares), corn stover + switchgrass + hybrid poplar (circles), and corn stover + switchgrass + *Miscanthus* (diamonds). The dashed lines are linear fits to the individual yield loci.

All of the flow parameters for the three feedstock blends are quite similar across the tested pre-shear normal stress values (Table 5). The average flowability indices of the CS + SG, CS + SG + HP, CS + SG + MIS blends are 5.6 ± 1.3, 5.6 ± 1.1, and 6.1 ± 1.4; while the average ϕ_i values for the blended feedstocks are 39.1 ± 1.3, 37.4 ± 1.9, and 35.8 ± 1.7, respectively.

The flow properties of the blends appear to be a composite of their individual pure feedstock constituents. When the angle of internal friction (ϕ_i) and cohesion (τ_0) at a pre-shear normal stress of 9 kPa for the blended feeds are plotted with the pure feedstocks (Fig. 9), the blends fall between the highest and lowest ϕ_i and τ_0 values. The bars in Fig. 9 represent measured data, while the square and circle symbols are calculated values of ϕ_i and τ_0, respectively, for the blendstocks based on the measured values of their individual "pure" components. The calculated values of ϕ_i and τ_0 overlap near perfectly with the measured values (Fig. 9). As a result, it appears that the individual feedstock flow properties can be measured separately and based on the blending ratio, the flowability characteristics of the feedstock blends can be predicted.

Broadening the scope of Fig. 9, the average flowability indices of the pure and blended feedstocks across all of the measured pre-shear normal stresses (3, 6, 9, and 15 kPa) were evaluated (Fig. 10). Again, the ff_c values of the blends fell within upper and lower bounds of the flowability indices of the pure feedstocks. Also, the calculated values of ff_c (circles) for the blendstocks agree with the measured data (bars; Fig. 10). The computed ff_c values for the binary (CS + SG) and two ternary blends (CS + SG + HP and CS + SG + MIS) fell within a single standard deviation of the measured values. Although the binary blend (CS + SG) calculated flow index is slightly larger than the experimental value. This discrepancy is most likely caused by the large fluctuation in the measured flowability index value for pure SG, which ranges from ~7.5–10.6. The large variance in switchgrass' ff_c value is compounded by the fact that it makes up 50% by weight of the binary blend and only 33% of the ternary blends. Thus, the wide-ranging flow index for SG has a greater impact on the predicted value of the binary blend in comparison to the ternary blends.

In general, the flow measurements of the blended feedstocks agree with the flowability data from their pure feedstock constituents. If the pure feedstocks flow properties are thoroughly and reliably interrogated, then the flow properties of the blended feedstocks can be predicted arithmetically. Therefore, only the flowability of the individual feedstocks need to be measured and the blend characteristics can be inferred; giving engineers the ability to design feedstock blend ratios based on desired flow characteristics. This novel outcome has the

Table 5
Shear testing results for the blended feedstocks at pre-shear normal stress (N_c) values of 3, 6, 9, and 15 kPa (unconfined yield stress (f_c), major and minor principal stresses (σ_1 and σ_2, respectively), cohesion (τ_0), static and effective angles of interparticle friction (ϕ_i and ϕ_e, respectively), and flowability index (ff_c)).

Material	N_c (kPa)	f_c (kPa)	σ_1 (kPa)	σ_2 (kPa)	τ_0 (kPa)	ϕ_i (°)	ϕ_e (°)	ff_c (−)
CS + SG	3	1.3 ± 0.3	6.9 ± 0.3	1.3 ± 0.1	0.32 ± 0.10	37.7 ± 2.8	42.0 ± 1.6	5.3 ± 1.5
	6	2.7 ± 0.4	14.6 ± 0.9	2.5 ± 0.2	0.62 ± 0.12	40.1 ± 2.5	44.1 ± 1.9	5.5 ± 0.8
	9	4.3 ± 0.9	21.2 ± 0.7	3.8 ± 0.1	1.03 ± 0.24	39.1 ± 1.3	43.9 ± 0.6	4.9 ± 1.0
	15	8.2 ± 0.1	36.1 ± 0.4	5.4 ± 0.1	1.82 ± 0.03	42.2 ± 0.3	47.5 ± 0.3	4.4 ± 0.1
CS + SG + HP	3	1.1 ± 0.1	6.7 ± 0.1	1.3 ± 0.1	0.28 ± 0.02	37.9 ± 2.1	42.0 ± 1.9	5.8 ± 0.3
	6	2.2 ± 0.4	14.4 ± 0.7	2.4 ± 0.1	0.49 ± 0.11	41.7 ± 2.6	45.0 ± 1.8	6.6 ± 1.6
	9	4.7 ± 0.6	21.1 ± 1.5	4.0 ± 0.3	1.16 ± 0.11	37.4 ± 1.9	42.8 ± 2.1	4.5 ± 0.3
	15	6.0 ± 0.5	30.2 ± 0.8	5.9 ± 0.2	1.54 ± 0.15	36.0 ± 4.0	40.7 ± 3.8	5.0 ± 0.3
CS + SG + MIS	3	0.8 ± 0.2	6.0 ± 0.4	1.3 ± 0.1	0.22 ± 0.05	35.2 ± 1.7	38.4 ± 1.7	7.2 ± 1.1
	6	2.2 ± 0.5	13.9 ± 1.1	2.6 ± 0.2	0.53 ± 0.17	36.0 ± 2.7	41.2 ± 1.6	6.3 ± 0.8
	9	2.9 ± 0.6	18.8 ± 1.2	4.1 ± 0.3	0.74 ± 0.17	35.8 ± 1.7	39.5 ± 0.8	6.5 ± 1.3
	15	5.8 ± 0.6	31.8 ± 0.4	5.7 ± 0.1	1.53 ± 0.15	38.5 ± 0.8	43.2 ± 0.8	5.5 ± 0.4

capability to save feedstock handling engineers and scientists significant time and money when investigating prospective feedstock blends.

3.3.3. Wall friction

Wall friction testing involves measuring a wall yield locus, which describes the shear stress required to move granular solids continuously across a wall surface under a specified normal stress. From the wall yield loci, wall friction coefficients (or angles) can be determined. All of the measured coefficients of wall friction (at a surface roughness, Ra, of 1.2 μm) for the pure and blended feedstocks ranged from ~0.16 to 0.20 (Fig. 11). A coefficient of wall friction of around 0.17 (or an angle of ~10) is considered relatively low. Thus, none of these materials, pure or blended, should display large wall binding affinities under low or moderate consolidation stresses. However, under large consolidation stress values (like the ones observed during pelleting) the wall friction coefficients are still significant enough to generate resistance during extrusion.

3.4. Pelleting pressure calculation

A conventional pelleting process involves pushing granular material through a cylindrical die. The friction between the compacted material and the die wall creates resistance to material flow through the die. Thus, the pelleting process can be broken down into two simple steps. First, ground (or "loose") biomass is compressed into a densified plug. Secondly, the densified biomass plug is forced through a pellet die to form cylindrical pellets with fixed dimensions. There will be an energy cost associated with compressing the material, as well as an energy requirement for extrusion through the die. Commonly, pelleting dies are tapered and the compression and extrusion steps occur simultaneously. However, for simplification, they are treated as separate stages in this study.

The flow of densified biomass through a pelleting die is analogous to plug-flow of a Newtonian fluid in a pipe. Ignoring gravitational effects and density fluctuations, and assuming the flow is steady, fully-developed, and one-directional, the Navier–Stokes conservation of momentum in cylindrical coordinates can be reduced to:

$$0 = \frac{1}{r}\frac{\partial(r\tau_{rz})}{\partial r} - \frac{\partial P}{\partial z}; \tag{1}$$

where τ_{rz} is the shear stress acting in the r-direction as a result of material flowing in the z-direction; while $\partial P/\partial z$ represents the pressure drop across the length of the pelleting die. Because τ_{rz} depends on r only and P depends on z only, the two terms in Eq. (1) must equal a constant (A_1). Therefore, an expression for τ_{rz} can be obtained independently from P:

$$\frac{1}{r}\frac{\partial(r\tau_{rz})}{\partial r} = A_1. \tag{2}$$

The boundary conditions for τ_{rz} are:

1) when $r = 0$, $\partial\tau_{rz}/\partial r = 0$,
2) when $r = R$, $\tau_{rz} = \mu_w P_w$.

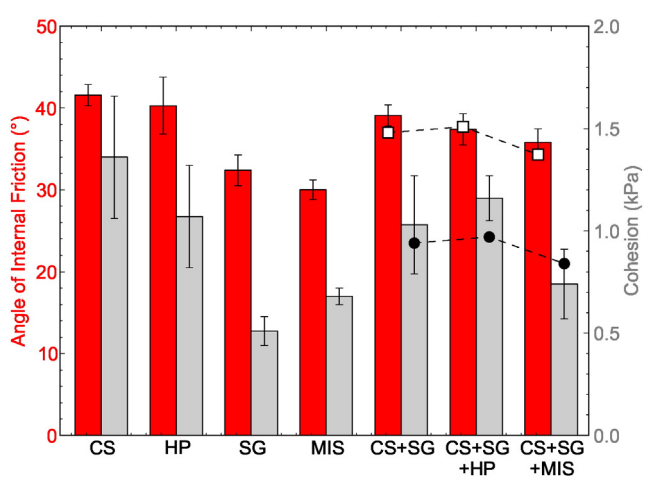

Fig. 9. Angle of internal friction (left axis) and interparticle cohesion (right axis) at a pre-shear normal stress of 9 kPa for both the pure and blended feedstocks (bar charts). The symbols represent a weighted average angle of internal friction (squares) and cohesion (circles) for the blended feedstocks based on their composition. The dashed lines connecting the symbols are to guide the eye.

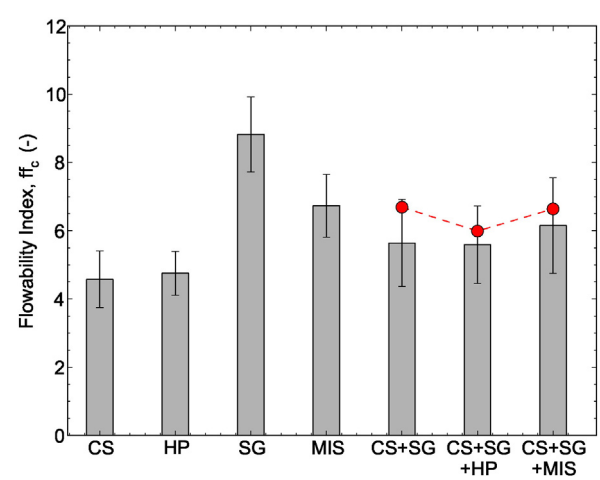

Fig. 10. Average flowability indices for both the pure and blended feedstocks across all tested pre-shear normal stress values (3, 6, 9, and 15 kPa) (bar chart). The symbols represent a weighted average flowability for the blended feedstocks based on their composition. The dashed lines connecting the symbols are to guide the eye.

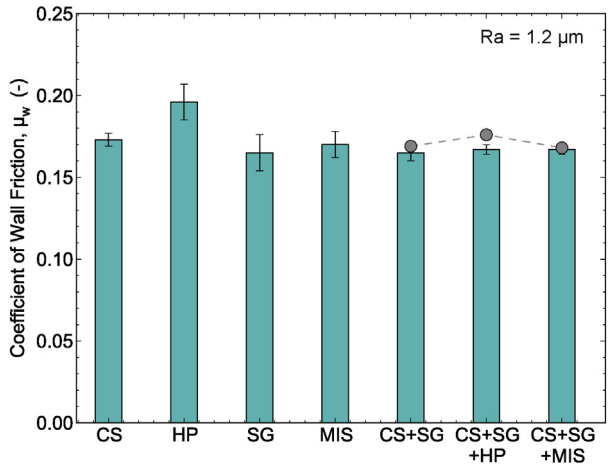

Fig. 11. Average coefficients of wall friction (Ra = 1.2 μm) across pre-shear normal stress values of 3, 9, and 15 kPa for both the pure and blended feedstocks (bar chart). The symbols represent a weighted average wall friction coefficients for the blended feedstocks based on their composition. The dashed lines connecting the symbols are to guide the eye.

μ_w is the coefficient of friction between the die wall and the biomass plug (i.e., the coefficient of wall friction; Fig. 11) and P_w is the resultant stress acting on the die wall due to the axial force driving biomass through the die. After applying the boundary conditions, A_1 was found to be:

$$A_1 = \frac{2\mu_w P_w}{R}. \tag{3}$$

With a fully-defined A_1, Eq. (1) now becomes:

$$\frac{\partial P}{\partial z} = \frac{2\mu_w P_w}{R}. \tag{4}$$

However, P_w is a function of P and thus, Eq. (4) cannot be integrated in its current form. Fortunately, P_w is simply defined as:

$$P_w = \kappa P, \tag{5}$$

where κ is the radial-to-axial stress proportionality constant (commonly denoted as λ); which is simply the ratio of the minor and major principal stress values (Table 6).

The boundary condition for P is: when $z = 0$, $P = P_c$; where P_c is the pressure required to compress the "loose" biomass to the desired pellet density. Values for P_c were obtained from the logarithmic fits of the compressibility data in Figs. 4 and 5. These expressions were then extrapolated to the degree of compression required to pellet each material (C_p; Table 6):

$$C_P = \frac{\rho_P - \rho_G}{\rho_P} \cdot 100\%, \tag{6}$$

Table 6
Energy and pressure requirements for pelleting the pure and blended feedstocks.

Material	κ (−)	C_P (%)	P_C (MPa)	P_P (MPa)	E_C (kWh/t)
CS	0.15	84	15	53	88
HP	0.17	82	58	192	107
SG	0.25	79	196	1003	146
MIS	0.24	78	239	1727	293
CS + SG	0.19	80	96	266	79
CS + SG + HP	0.17	83	63	214	100
CS + SG + MIS	0.20	79	41	147	78

where ρ_P and ρ_G are the pellet and ground (or "loose") bulk densities, respectively (Table 1). Using the boundary condition, Eq. (4) can be separated and integrated to obtain:

$$P = P_C \, exp\left(\frac{2\mu_w \kappa z}{R}\right). \tag{7}$$

The overall pelleting pressure (P_P) required to compress "loose" biomass into a densified plug and then force it through a pelleting die of length L and diameter D is:

$$P_P = P_C \, exp(4\mu_w \kappa L/D). \tag{8}$$

Using Eq. (8) and the compressibility, shear cell, and wall friction data, the pressure required to pellet (P_P) the pure and blended feedstocks could be obtained. The calculated P_P values ranged from 50 to 1700 MPa for the pure feedstocks and 145 to 270 MPa for the blended feedstocks (Table 6). The calculated pelleting pressures for CS and HP and the three blendstocks are equivalent to typical pressures used to pellet herbaceous straws and grasses, as well as wood residues (~20–150 MPa) [9,21,20,5]. The SG and MIS feedstocks, on the other hand, had abnormally high calculated pelleting pressures (>900 MPa). However, relatively large pressures (300–800 MPa) have been used previously to densify biomass materials [43].

The calculated pelleting pressure values were then compared to the measured pelleting energy consumption from Table 1 (Fig. 12). Remarkably, there is strong agreement between the measured energy consumption and pelleting pressure values. The materials that required more energy for pelleting, switchgrass and *Miscanthus*, also had large pelleting pressure requirements: 1003 and 1727 MPa, respectively. While the materials requiring low energy for pelleting, corn stover, hybrid poplar, and the three blendstocks, also had relatively low calculated pelleting pressures (50–270 MPa).

The total pelleting pressure (P_P), as well as the compression pressure (P_C) are listed for the four pure feedstocks and the three blends in Table 6. Roughly 40 to 15% of the pelleting pressure was used to compress the materials and the remaining 60 to 85% was used to overcome friction in the pelleting die. At first glance, the extrusion pressure (the difference between P_P and P_C) seems disproportionately large. Our expectation was that the force required to compress the materials would makeup the majority of the energy involved in the pelleting process. However, Mewes [44] studied the consumption of energy to overcome

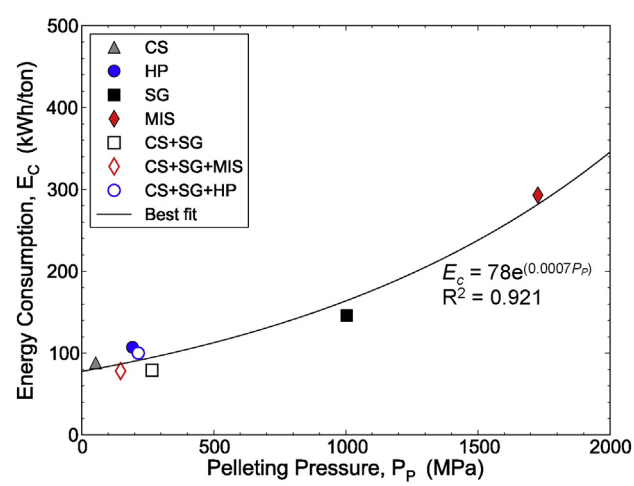

Fig. 12. Electrical pelleting energy consumption (E_C) versus the calculated pelleting pressure (P_P) for pure feedstocks of corn stover (filled triangle), hybrid poplar (filled circle), switchgrass (filled square), *Miscanthus* (filled diamond), and blended feedstocks of corn stover + switchgrass (open square), corn stover + switchgrass + hybrid poplar (open circle), and corn stover + switchgrass + *Miscanthus* (open diamond). The solid line is an exponential (best) fit to the data.

friction during compression of straw and hay and showed that roughly 40% of the total applied energy was used to compress the materials (straw and hay), while the remaining 60% was used to overcome friction. Additionally, Mani et al. [45] showed that over 50% of the energy for briquetting corn stover was due to friction during extrusion. Mani et al. also showed that when the briquetting pressure was increased from 5 to 15 MPa, the ratio of the extrusion to compression energy increased; which they attributed to the increase in normal pressure between the die and the briquette. Therefore, it is reasonable to assume that during pelleting, which occurs at higher pressures than briquetting (>30 MPa), the extrusion energy could account for 60 to 80% of the total energy requirements.

The development and validation of the pelleting pressure model (Eq. (8)) allows for materials to be "pre-screened" prior to pelleting. A feedstock's material properties (specifically compressibility, shear, and wall friction) can be measured and its pelleting feasibility can be assessed without actually having to pellet the material; saving biomass process and handling engineers substantial amounts of time and money.

4. Conclusions

The flow properties (compressibility, shear, and wall friction) of "pure" and blended biomass feedstocks were evaluated and compared to measured pelleting energy consumption values. As projected, the compressibilities of the biomass feedstocks were directly correlated with their pelletization energies. However, a feedstock's flow properties (i.e., the material's cohesion, yield strength, interparticle friction) were found to be inversely related to its pelleting energy requirements. In addition, the compressibility and flowability of a feedstock blend can be predicted by averaging the measured properties of its pure feedstock constituents; thus, only the flow parameters of the pure components need to be directly measured. A model was also developed to calculate the required pressure to pellet the pure and blended biomass species. Strong correlation was observed between the measured pelleting energy consumption values and the predicted pelleting pressure. This model allows for a feedstock's pelleting suitability to be assessed, based on its compressibility, flowability, and wall friction, without actually having to pelletize the material. Overall, the results reported here will help guide ongoing feedstock formulation efforts, while also enhancing pelleting process efficiency.

Acknowledgments

This work was funded by the U.S. Department of Energy under Contract No. DE-AC36-08-GO28308 with the National Renewable Energy Laboratory and through the BioEnergy Technologies Office. The authors thank Dave Pace, Marnie Cortez, Craig Conner, and Austin Matthews for their valued technical assistance.

References

[1] C.E. Wyman, Cellulosic ethanol: a unique sustainable liquid transportation fuel, MRS Bull. 33 (4) (2008) 381–383, http://dx.doi.org/10.1557/mrs2008.77.
[2] A.A. Modenbach, S.E. Nokes, Enzymatic hydrolysis of biomass at high-solids loadings — a review, Biomass Bioenergy 56 (2013) 526–544, http://dx.doi.org/10.1016/j.biombioe.2013.05.031.
[3] J.S. Tumuluru, C.T. Wright, J.R. Hess, K.L. Kenney, A review of biomass densification systems to develop uniform feedstock commodities for bioenergy application, Biofuels Bioprod. Biorefin. 5 (6) (2011) 683–707, http://dx.doi.org/10.1002/bbb.324.
[4] N. Kaliyan, R.V. Morey, Factors affecting strength and durability of densified biomass products, Biomass Bioenergy 33 (3) (2009) 337–359, http://dx.doi.org/10.1016/j.biombioe.2008.08.005.
[5] S. Mani, L.G. Tabil, S. Sokhansanj, Effects of compressive force, particle size and moisture content on mechanical properties of biomass pellets from grasses, Biomass Bioenergy 30 (7) (2006) 648–654, http://dx.doi.org/10.1016/j.biombioe.2005.01.004.
[6] S. Mani, L. Tabil, S. Sokhansanj, Grinding performance and physical properties of wheat and barley straws, corn stover and switchgrass, Biomass Bioenergy 27 (4) (2004) 339–352, http://dx.doi.org/10.1016/j.biombioe.2004.03.007.
[7] D. Inman, N. Nagle, J. Jacobson, E. Searcy, A.E. Ray, Feedstock handling and processing effects on biochemical conversion to biofuels, Biofuels Bioprod. Biorefin. 4 (5) (2010) 562–573, http://dx.doi.org/10.1002/bbb.241.
[8] L. Tabil, P. Adapa, M. Kashaninejad, Biomass feedstock pre-processing — part 2: densification, in: D.M.A.D.S. Bernardes (Ed.), Biofuel's Engineering Process Technology, InTech 2011, pp. 439–464, http://dx.doi.org/10.5772/18495 (Ch. 19).
[9] P. Adapa, L. Tabil, G. Schoenau, Compaction characteristics of barley, canola, oat and wheat straw, Biosyst. Eng. 104 (3) (2009) 335–344, http://dx.doi.org/10.1016/j.biosystemseng.2009.06.022.
[10] P.K. Adapa, L.G. Tabil, G.J. Schoenau, Compression characteristics of non-treated and steam-exploded barley, canola, oat, and wheat straw grinds, Appl. Eng. Agric. 26 (4) (2010) 617–632.
[11] S. Mani, L. Tabil, S. Sokhansanj, Evaluation of compaction equations applied to four biomass species, Can. Biosyst. Eng. 46 (3) (2004) 3.55–3.61.
[12] M. Kashaninejad, L.G. Tabil, Effect of microwave-chemical pre-treatment on compression characteristics of biomass grinds, Biosyst. Eng. 108 (1) (2011) 36–45, http://dx.doi.org/10.1016/j.biosystemseng.2010.10.008.
[13] J.M. Wilson, L.J. McKinney, K. Theerarattananoon, T.C. Ballard, D. Wang, S.A. Staggenborg, P.V. Vadlani, Energy cost for pelleting and transportation of selest cellulosic biomass feedstocks for ethanol production, Appl. Eng. Agric. 30 (1) (2014) 77–85.
[14] K. Theerarattananoon, F. Xu, J. Wilson, R. Ballard, L. Mckinney, S. Staggenborg, P. Vadlani, Z.J. Pei, D. Wang, Physical properties of pellets made from sorghum stalk, corn stover, wheat straw, and big bluestem, Ind. Crop. Prod. 33 (2) (2011) 325–332, http://dx.doi.org/10.1016/j.indcrop.2010.11.014.
[15] J.R. Hess, C.T. Wright, K.L. Kenney, Cellulosic biomass feedstocks and logistics for ethanol production, Biofuels Bioprod. Biorefin. 1 (3) (2007) 181–190, http://dx.doi.org/10.1002/bbb.26.
[16] P. Krishnakumar, K.E. Ileleji, A comparative analysis of the economics and logistical requirements of different biomass feedstock types and forms for ethanol production, Appl. Eng. Agric. 26 (5) (2010) 899–907 (annual Meeting of the American-Society-of-Agricultural-and-Biological-Engineers, Reno, NV, Jun 21–24, 2009).
[17] K.L. Kenney, W.A. Smith, G.L. Gresham, T.L. Westover, Understanding biomass feedstock variability, Biofuels 4 (1) (2013) 111–127, http://dx.doi.org/10.4155/bfs.12.83.
[18] D.L. Carpenter, R.L. Bain, R.E. Davis, A. Dutta, C.J. Feik, K.R. Gaston, W. Jablonski, S.D. Phillips, M.R. Nimlos, Pilot-scale gasification of corn stover, switchgrass, wheat straw, and wood: 1. Parametric study and comparison with literature, Ind. Eng. Chem. Res. 49 (4) (2010) 1859–1871, http://dx.doi.org/10.1021/ie900595m.
[19] P. Das, A. Ganesh, P. Wangikar, Influence of pretreatment for deashing of sugarcane bagasse on pyrolysis products, Biomass Bioenergy 27 (5) (2004) 445–457, http://dx.doi.org/10.1016/j.biombioe.2004.04.002.
[20] C. Ndiema, P. Manga, C. Ruttoh, Influence of die pressure on relaxation characteristics of briquetted biomass, Energy Convers. Manag. 43 (16) (2002) 2157–2161, http://dx.doi.org/10.1016/S0196-8904(01)00165–0.
[21] Y. Li, H. Liu, High-pressure densification of wood residues to form an upgraded fuel, Biomass Bioenergy 19 (3) (2000) 177–186, http://dx.doi.org/10.1016/S0961-9534(00)00026-X.
[22] O. Fasina, S. Sokhansanj, Effect of fines on storage and handling properties of alfalfa pellets, Can. Agric. Eng. 38 (1) (1996) 25–29.
[23] Z. Colley, O.O. Fasina, D. Bransby, Y.Y. Lee, Moisture effect on the physical characteristics of switchgrass pellets, Trans. ASABE 49 (6) (2006) 1845–1851.
[24] O.O. Fasina, Physical properties of peanut hull pellets, Bioresour. Technol. 99 (5) (2008) 1259–1266, http://dx.doi.org/10.1016/j.biortech.2007.02.041.
[25] P.K. Adapa, L.G. Tabil, G.J. Schoenau, Factors affecting the quality of biomass pellet for biofuel and energy analysis of pelleting process, Int. J. Agric. Biol. Eng. 6 (2) (2013) 1–12, http://dx.doi.org/10.3965/j.ijabe.20130602.001.
[26] E. Monedero, H. Portero, M. Lapuerta, Pellet blends of poplar and pine sawdust: effects of material composition, additive, moisture content and compression die on pellet quality, Fuel Process. Technol. 132 (0) (2015) 15–23, http://dx.doi.org/10.1016/j.fuproc.2014.12.013.
[27] N. Yancey, C. Wright, C. Conner, J. Tumuluru, Optimization of preprocessing and densification of sorghum stover at full-scale operation, Proceedings of the ASABE 2011 Annual International Meeting.
[28] International organization for standardization, ISO Standard 9276-2:2014 — Representation of Results of Particle Size Analysis — Part 2: Calculation of Average Particle Sizes/Diameters and Moments From Particle Size Distributions, May 2014.
[29] R. Trottier, S. Dhodapkar, A guide to characterizing particle size and shape, Chem. Eng. Prog. 110 (7) (2014) 36–46.
[30] R. Freeman, Measuring the flow properties of consolidated, conditioned and aerated powders — a comparative study using a powder rheometer and a rotational shear cell, Powder Technol. 174 (1–2) (2007) 25–33, http://dx.doi.org/10.1016/j.powtec.2006.10.016 (pSA Conference 2003, Harrogate, England, 2003).
[31] R.E. Freeman, J.R. Cooke, L.C.R. Schneider, Measuring shear properties and normal stresses generated within a rotational shear cell for consolidated and non-consolidated powders, Powder Technol. 190 (1–2) (2009) 65–69, http://dx.doi.org/10.1016/j.powtec.2008.04.084 (symposium on Powder Science and Technology - Powders and Sintered Material, Albi, France, MAY 23-25, 2007).
[32] A.W. Jenike, Storage and Flow of Solids, Salt Lake City, Utah, 1964.
[33] J.W. Carson, H. Wilms, Development of an international standard for shear testing, Powder Technol. 167 (1) (2006) 1–9, http://dx.doi.org/10.1016/j.powtec.2006.04.005.
[34] J. Tomas, H. Schubert, Particle characterization, Partec 79 (1979) 301–319.
[35] O.O. Fasina, Flow and physical properties of switchgrass, peanut hull, and poultry litter, Trans. ASABE 49 (3) (2006) 721–728.

[36] G. Barbosa-Canovas, P. Juliano, Compression and Compaction Characteristics of Selected Food Powders, 49, Kluwer Academic Plenum Publishers, New York, NY, 2005http://dx.doi.org/10.1016/S1043-4526(05)49006–3.
[37] V. Ganesan, K.A. Rosentrater, K. Muthukurnarappan, Flowability and handling characteristics of bulk solids and powders — a review with implications for DDGS, Biosyst. Eng. 101 (4) (2008) 425–435, http://dx.doi.org/10.1016/j.biosystemseng.2008.09.008.
[38] S. Kokova, N. Pilpel, The failure properties of lactose and calcium carbonate powders, Powder Technol. 5 (1971) 329–343.
[39] P. Chen, Z. Yuan, X. Shen, Y. Zhang, Flow properties of three fuel powders, Particuology 10 (4) (2012) 438–443, http://dx.doi.org/10.1016/j.partic.2011.11.013.
[40] M. Gil, D. Schott, I. Arauzo, E. Teruel, Handling behavior of two milled biomass: Srf poplar and corn stover, Fuel Process. Technol. 112 (2013) 76–85, http://dx.doi.org/10.1016/j.fuproc.2013.02.024.
[41] F. Miccio, D. Barletta, M. Poletto, Flow properties and arching behavior of biomass particulate solids, Powder Technol. 235 (2013) 312–321, http://dx.doi.org/10.1016/j.powtec.2012.10.047.
[42] N. Chevanan, A.R. Womac, V.S.R. Bitra, D.C. Yoder, S. Sokhansanj, Flowability parameters for chopped switchgrass, wheat straw and corn stover, Powder Technol. 193 (1) (2009) 79–86, http://dx.doi.org/10.1016/j.powtec.2009.02.009.
[43] A. Demirbas, A. Sahin, Evaluation of biomass residue 1. briquetting waste paper and wheat straw mixtures, Fuel Process. Technol. 55 (2) (1998) 175–183, http://dx.doi.org/10.1016/S0378-3820(98)00041–1.
[44] E. Mewes, Compression relationships as a result of experiments in pressure chambers, Landwirtsch. Forsch. 9 (3) (1959) 68–76.
[45] S. Mani, L. Tabil, S. Sokhansanj, Specific energy requirement for compacting corn stover, Bioresour. Technol. 97 (12) (2006) 1420–1426, http://dx.doi.org/10.1016/j.biortech.2005.06.019.